Supplementary Material A: Summary of field data used in the study.

Table SMA – Characteristics (source, LON (longitude), LAT (latitude), time frame, and sampling frequency) of the field sampling sites.

Source – Variable (Station)	LON [°]	LAT [°]	Time frame	Sampling frequency
MAGEST – Turbidity (Le Verdon)	-1.0421	45.5438	2017 – 2021	10-30 min
MAGEST – Turbidity (Pauillac)	-0.7426	45.1985	2017 – 2018	10-30 min
GEMMES – Turbidity (buoy 20)	-1.3917	45.6375	2016/11 – 2017/09	15 min
HydroEAU – River discharge (Garonne, Dordogne)			1959 – 2021	daily
Meteo France – Wind (Cap Ferret)	-1.2480	44.3160	1985 – 2022	3-hourly
Meteo France – Wind (Royan)	-0.9683	45.6317	1991 – 2022	hourly
Meteo France – Wind (Pauillac)	-0.7828	45.2142	2004 – 2020	hourly
Meteo France – Wind (Merignac/Bordeaux)	-0.6900	44.8300	2004 – 2020	hourly

Supplementary Material B: Comparativeness of satellite derived turbidity and field stations

Match-ups between Sentinel-3/OLCI and field turbidity data were identified originating from satellite overpasses quality-controlled for flags caused by clouds or other atmospheric interferences. Water reflectance of regions of satellite scenes with flags indicating such artifacts were removed and not considered for match-ups. From these match-ups, an empirical algorithm was established aided by a Support Vector Machine (SVM) model. The comparison between turbidity estimates using the red and near infra-red bands (Figure SMA) resulted in good agreement with field turbidity: $r_{kendal\text{-}t} = 0.72$, p-value << 0.0001; n = 174.

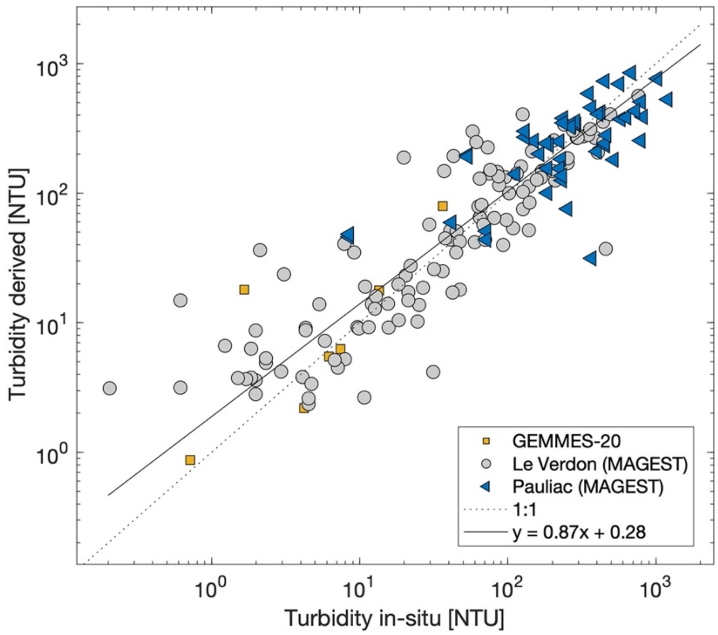

Figure SMB –Type-II linear regression (black line) between field turbidity and Sentinel-3 derived turbidity. Blue-triangle symbols represent field turbidity from Pauillac station, Light-gray symbols represent field turbidity from Le Verdon station and Yellow-squared symbol represents field data from the GEMMES network in buoy 20. Dashed grey line is 1:1.

Supplementary Material C: Comparativeness and bias correction of wind from ERA5 (ECMWF)

To overcome systematic errors from reanalysis ECMWF ERA-5 wind speeds, we performed a bias correction by applying the Cumulative Distribution Function (CDF) matching approach (https://nl.mathworks.com/matlabcentral/fileexchange/78784-cdf-matching-bias-correction-method-in-matlab; accessed on August, 2023, by Singh et al., 2020 and Reichle & Koster, 2004) for the years between 2005 and 2021. This is one of the widely used statistical methods to minimise the bias in a derived or modelled data compared with a more reliable source of data (usually field). We adjusted the ECMWF wind speed (u and v components) according to the CDF of field wind speeds to minimise their difference. The data was fit to a polynomial function of 3rd order ($y = p_1 (x^3) + p_2 (x^2) + p_3 (x^1) + p_4$), then bias corrected with the coefficients shown in Table SM3.

Table SMC – Coefficients estimated from CDF matching for BIAS correction.

Wind component	p_1	p_2	p_3	p_4
u	-0.000367	0.0153	-0.1101	-0.1366
v	-0.001600	0.0049	-0.0302	0.2107

Figure SMC-a,b shows the reference (field data), the biased and the bias-corrected wind speed distribution.

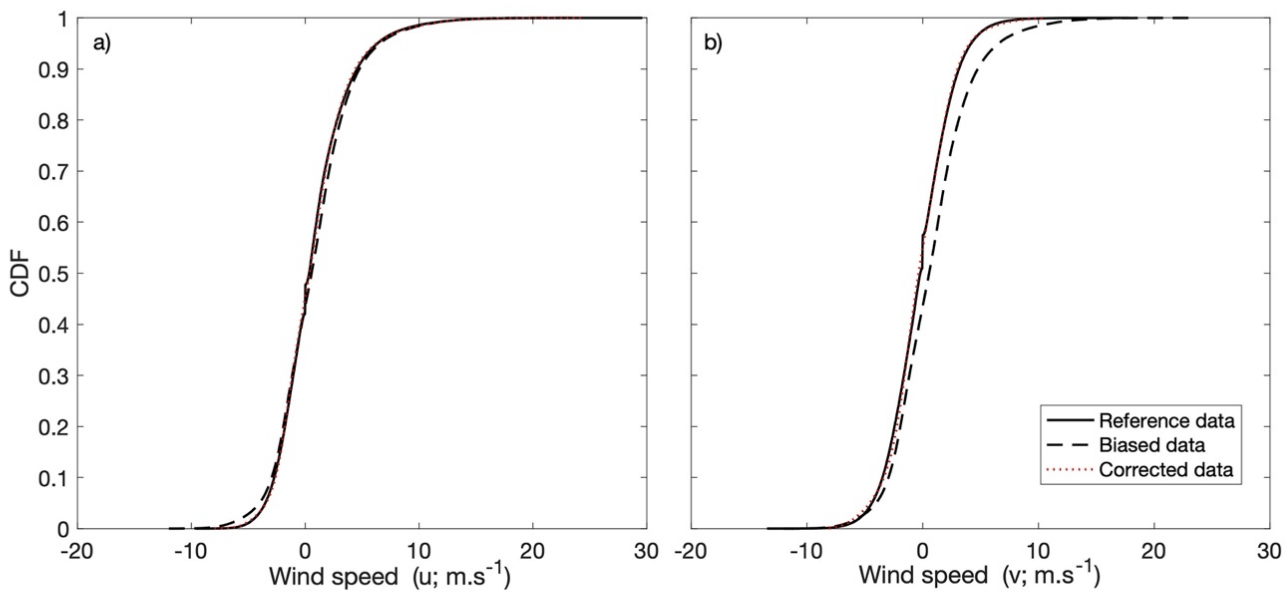

Figure SMC – Bias correction using the CDF matching technique. Solid black line is the CDF of field measured wind speed for u (a) and v (b) wind speed components, dashed and dotted lines are the CDF of biased and bias-corrected wind speed from reanalysis ERA-5 ECMWF data, respectively

33 **Supplementary Material D: Maximum wind speeds**

34 Spatial distribution of maximum winds speeds from ECMWF-ERA5 bias corrected wind speeds, and field wind 35 speeds.

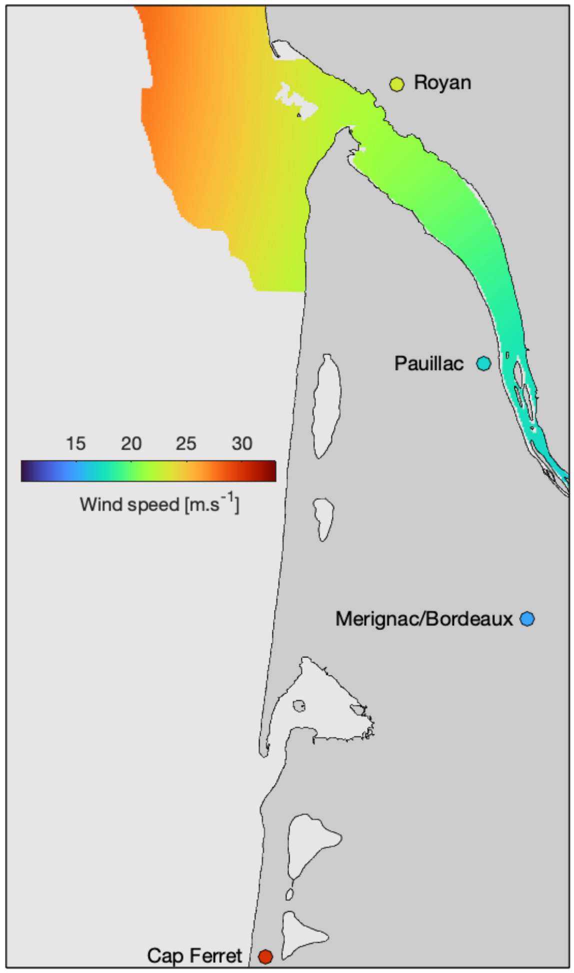

36

37 Figure SMD – Maximum wind speeds of the time series of bias corrected ECMWF ERA5 (2016 to 2021) and 38 field data at stations Cap Ferret, Merignac/Bordeaux, Pauillac and Royan with timeseries constrained between 39 years 2016 and 2021. Of the four field stations, stations Pauillac and Merignac/Bordeaux extend until 2020.

Supplementary Material E: Statistic metrics of non-parametric tests Kruskal-Wallis and Dunn-Sidak

The non-parametric test Kruskal-Wallis H tests the null hypothesis (H_0) that the data in each column of a matrix comes from the same distribution. The alternative hypothesis is that not all samples come from the same distribution. For database A and database B p-values were below 0.0001 for all hydro-sedimentological variables.

Building upon this, the Dunn-Sidak test was employed for pairwise comparisons to identify which specific groups of classes were statistically different. In the test, the null hypothesis (H_0) states that there is no difference between the ranks of the two classes being compared. If the *Q-value* exceeds the critical value, we reject H_0, indicating a statistically significant difference between the two classes. Conversely, if the *Q-value* is below the critical value, we fail to reject H_0, suggesting no significant difference between pair of hydro-sedimentological classes. Therefore, rejecting H_0 implies that the group being compared is statistically different from the other. If at least one variable (either river discharge, tidal current, water level, wind speed, depth or suspended sediment) for a given class is statistically significant different from the other classes, then that class is different from the remaining classes. Table SME-1 and Table SME-2, below, show the *Q-values* from the Dunn-Sidak tests for database A and database B, respectively.

Table SME-1 - Dunn-Sidak test results for Database A. The table presents the *Q-values* from pairwise group comparisons. Comparisons with *Q-values* in bold indicate that the null hypothesis cannot be rejected (*Q-value* < critical value of 3.25), suggesting no significant difference between the respective classes for a certain variable (river discharge, tidal current, water level, wind speed, depth or suspended sediment).

		C6	C3	C4	C7	C1	C5	C2	C8	C9	C10
River discharge	C6										
	C3	83.2									
	C4	50.3	65.8								
	C7	21026.0	15800.0	2991.8							
	C1	117.5	5.9	67.4	20711.0						
	C5	148.7	20.9	70.3	22547.0	20.1					
	C2	388.1	201.0	104.5	21889.0	259.4	262.9				
	C8	248.3	271.7	10.2	18388.0	348.4	390.5	593.9			
	C9	58.4	44.2	58.2	22491.0	68.2	97.7	356.3	312.1		
	C10	166.4	205.4	10.3	12488.0	236.2	255.1	395.8	**1.2**	203.6	
Tidal current	C6										
	C3	364.9									
	C4	40.1	109.4								
	C7	12241.0	9511.9	1730.9							
	C1	94.9	289.4	53.9	12083.0						
	C5	219.7	219.5	69.6	13257.0	113.4					
	C2	565.9	46.5	119.1	13078.0	456.4	380.4				
	C8	175.8	202.0	68.3	11022.0	88.7	6.4	318.4			
	C9	233.8	209.8	71.4	13290.0	127.1	14.9	366.8	18.4		
	C10	95.1	174.4	61.8	7460.9	36.9	28.3	236.7	22.5	36.2	

Table SME-1 - (continued)

		C6	C3	C4	C7	C1	C5	C2	C8	C9	C10
Water level	C6										
	C3	490.1									
	C4	57.6	36.3								
	C7	11471.0	9061.3	1717.2							
	C1	573.4	54.3	26.1	11802.0						
	C5	407.7	213.6	**3.0**	12623.0	212.3					
	C2	847.6	126.8	60.2	12569.0	242.7	489.0				
	C8	451.9	102.5	15.4	10613.0	64.6	120.2	285.0			
	C9	513.7	137.9	11.1	12745.0	109.8	113.5	381.7	28.7		
	C10	297.3	84.8	13.4	7199.3	51.7	70.9	198.4	7.4	10.9	
Wind speed	C6										
	C3	112.3									
	C4	83.7	104.5								
	C7	11741.0	8888.2	1615.0							
	C1	188.9	30.7	111.3	11687.0						
	C5	92.6	49.6	96.3	12600.0	110.6					
	C2	377.9	164.1	136.6	12382.0	176.5	309.6				
	C8	102.3	24.4	100.0	10507.0	66.9	27.2	227.9			
	C9	275.9	315.2	47.0	12256.0	470.6	397.4	688.7	347.9		
	C10	157.6	218.3	45.2	6009.1	270.6	214.0	380.9	216.2	3.7	
Depth	C6										
	C3	122.8									
	C4	135.0	157.3								
	C7	1654.2	12487.0	2258.4							
	C1	182.6	132,2	161.6	16383.0						
	C5	210.4	278.8	107.0	17416.0	399.7					
	C2	326.1	115.2	180.6	17242.0	132.2	565.3				
	C8	4.9	118.0	133.8	14655.0	166.9	178.0	291.6			
	C9	141.9	229.4	116.2	17510.0	333.1	74.2	495.5	118.3		
	C10	88.8	165.1	111.7	9866.6	198.6	29.4	281.2	81.5	9.9	
Suspended sediment	C6										
	C3	38.1									
	C4	29.2	36.2								
	C7	10359.0	7780.9	1469.6							
	C1	102.2	42.1	44.6	10251.0						
	C5	385.9	238.8	80.9	11416.0	263.7					
	C2	530.2	351.3	103.2	11118.0	409.9	171.5				
	C8	133.7	69.2	50.6	9312.6	37.2	195.4	329.9			
	C9	242.4	135.2	61.6	11291.0	123.4	155.4	319.8	70.2		
	C10	168.8	121.8	68.3	6401.9	103.3	47.9	141.4	74.9	34.3	

Table SME-2 - Dunn-Sidak test results for Database B. The table presents the *Q-values* from pairwise group comparisons. Comparisons with *Q-values* in bold indicate that the null hypothesis cannot be rejected (*Q-value* < critical value of 3.25), suggesting no significant difference between the respective classes for a certain variable (river discharge, tidal current, water level, wind speed, depth or suspended sediment). The symbol '-' indicates that the Dunn-Sidak test accepts the null hypothesis (*Q-value* ≤ critical value)

		C6	C3	C4	C7	C1	C5	C2	C8	C9	C10
River discharge	C6										
	C3	345.9									
	C4	207.3	554.8								
	C7	50.4	286.1	252.7							
	C1	36.2	395.0	178.2	87.4						
	C5	187.1	541.0	23.9	233.7	156.8					
	C2	43.8	353.6	143.0	88.4	12.6	123.5				
	C8	178.1	-	300.5	146.4	200.9	288.4	198.7			
	C9	25.2	202.4	164.3	9.2	49.3	149.6	54.9	130.2		
	C10	13.3	**1.8**	22.6	10.9	14.8	21.5	15.2	**0.2**	11.6	
Tidal current	C6										
	C3	479.6									
	C4	39.0	514.8								
	C7	191.9	271.9	228.3							
	C1	452.2	32.2	487.9	243.5						
	C5	350.8	124.7	386.8	149.2	94.1					
	C2	267.5	155.6	300.6	89.7	128.7	44.8				
	C8	163.4	113.7	186.0	47.2	95.9	41.8	11.9			
	C9	156.1	158.2	181.6	24.8	138.2	76.3	40.8	21.3		
	C10	-	19.7	**3.0**	7.6	18.4	14.3	12.1	11.2	24.8	
Water level	C6										
	C3	506.9									
	C4	154.6	343.5								
	C7	-	491.5	147.9							
	C1	299.2	217.4	136.5	288.6						
	C5	361.0	141.7	201.5	349.4	71.0					
	C2	281.9	165.3	140.7	273.8	22.5	39.4				
	C8	114.9	178.4	22.7	112.0	56.6	96.4	67.6			
	C9	173.0	159.1	68.4	169.0	20.8	66.2	35.0	31.7		
	C10	**0.6**	22.7	7.6	**0.8**	13.6	16.6	14.7	9.3	12.2	
Wind speed	C6										
	C3	127.9									
	C4	158.9	289.4								
	C7	94.0	28.7	248.6							
	C1	4.8	137.2	159.4	101.6						
	C5	62.3	193.0	98.7	155.7	59.6					
	C2	253.2	143.9	394.2	163.9	164.1	310.9				
	C8	35.0	109.6	59.5	91.0	32.6	**1.4**	193.5			
	C9	238.1	156.4	343.8	172.1	244.6	280.5	47.2	205.0		
	C10	15.6	10.0	22.8	11.3	15.8	18.3	**3.0**	18.2	**0.3**	

Table SME-2 - (continued)

		C6	C3	C4	C7	C1	C5	C2	C8	C9	C10
Depth	C6										
	C3	356.2									
	C4	71.6	425.9								
	C7	357.5	18.1	424.2							
	C1	40.8	410.4	33.5	408.5						
	C5	304.3	47.7	373.5	63.4	355.7					
	C2	319.3	7.4	381.1	8.8	364.0	49.1				
	C8	123.9	81.9	166.0	91.1	148.8	54.1	82.6			
	C9	206.6	25.8	253.7	37.3	236.3	5.3	29.4	49.0		
	C10	**2.7**	12.8	6.0	13.6	4.5	10.7	319.3	13.2	11.1	
Suspended sediment	C6										
	C3	169.7									
	C4	225.0	62.4								
	C7	255.3	95.6	33.0							
	C1	19.3	155.8	213.2	244.5						
	C5	335.2	172.3	105.0	70.0	327.0					
	C2	277.5	131.4	73.1	42.3	267.6	20.7				
	C8	67.1	30.9	66.7	86.3	56.7	129.3	110.8			
	C9	167.4	57.4	15.6	7.0	157.1	54.7	37.2	67.5		
	C10	5.8	13.2	16.0	17.5	6.6	20.6	19.6	10.9	17.0	

Supplementary Material F: Performance metrics of Random Forest algorithms by database and hydro-sedimentological class.

Table SMF-1 – Performance metrics of Random Forest algorithms in database A per class.

	Class	**R^2**	**RMSE $\log_{10}$[g.m^{-3}]**
Prevailing conditions	C6	0.93	0.0941
	C3	0.92	0.1104
	C4	0.91	0.1281
	C7	0.91	0.1116
	C5	0.91	0.1424
	C2	0.92	0.1331
Extreme events	C8	0.94	0.1537
	C9	0.94	0.1221
	C10	0.93	0.1425

Table SMF-2 – Performance metrics of Random Forest algorithms in database B per class.

	Class	**R^2**	**RMSE $\log_{10}$ [g.m^{-3}]**
Prevailing conditions	C6	0.94	0.0635
	C3	0.92	0.2054
	C4	0.95	0.0848
	C7	0.96	0.0697
	C5	0.92	0.1839
	C2	0.95	0.0979
Extreme events	C8	0.98	0.1222
	C9	0.96	0.0940
	C10	0.88	0.1013

Supplementary Material G: Satellite-based relative contribution to variability of turbidity (database B)

Relative contribution results using database B and the proposed hydro-sedimentary framework. Figure SMG-1 depicts spatial variability of relative contribution of forcings to turbidity, Figure SMG-2 shows the distributions of the 10 identified hydro-sedimentological classes, and Figure SMG-3 depict the class-specific relative contribution of forcings.

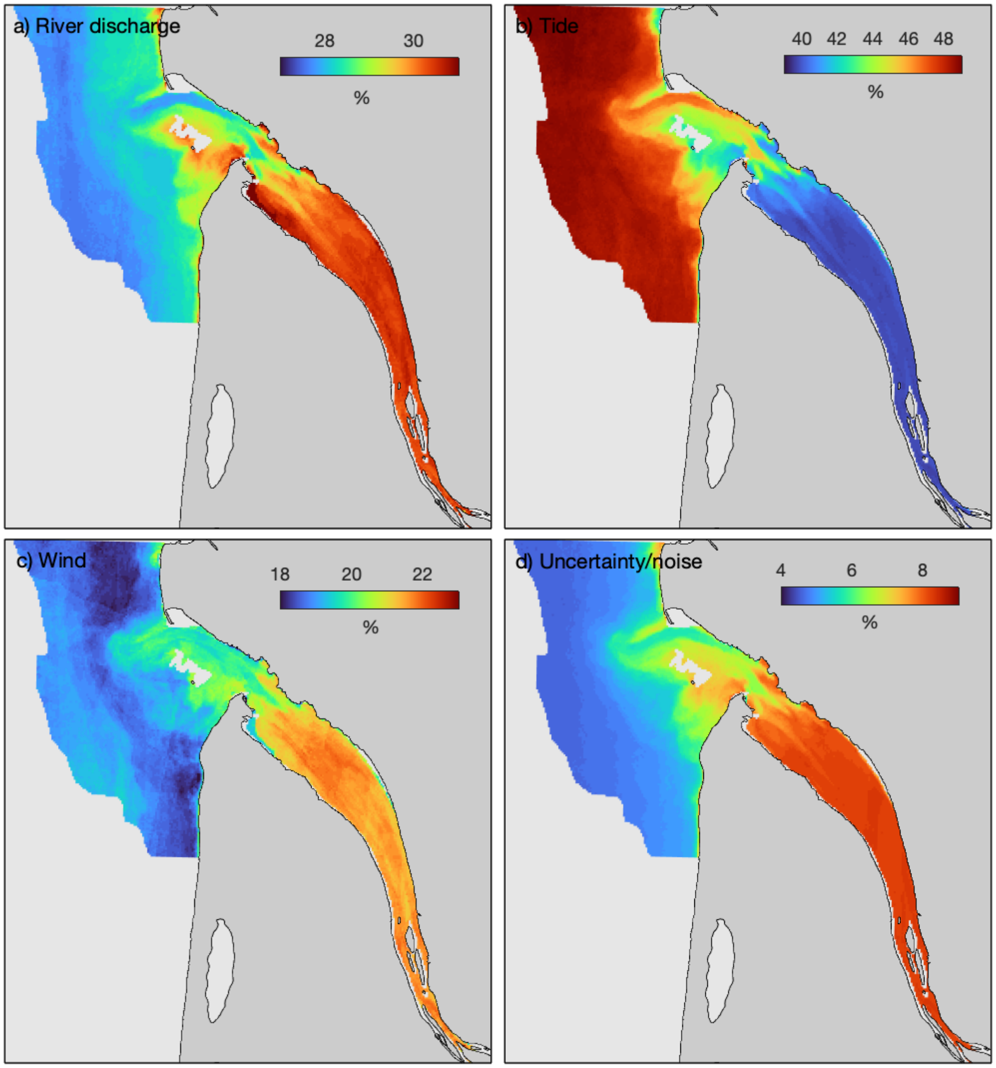

Figure SMG-1 - Synoptical mean contribution of predicting factors for satellite-derived turbidity (database B, with satellite-based turbidity): (a) river discharge, (b) tides, (c) winds and (d) uncertainties/noise. Attention to the different ranges of percentage on each subplot.

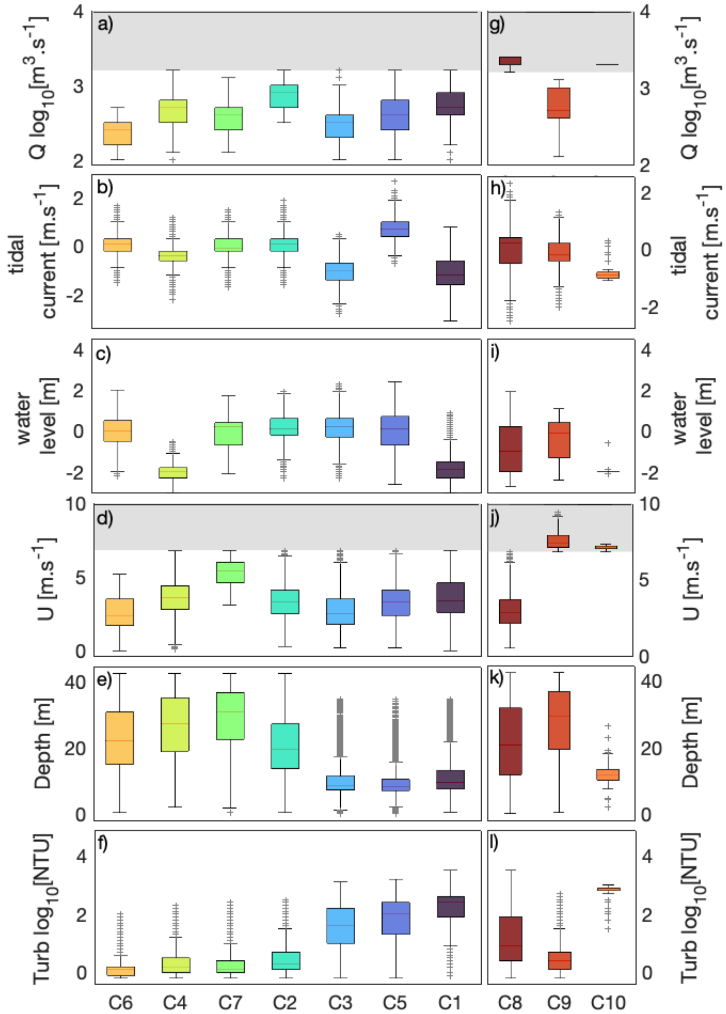

Figure SMG-2- Classes of coherent hydrodynamical and sedimentological patterns of database B (x-axis), for river discharge (a,g, $\log_{10}$ transformed), tidal current (b,h), water level (c,i), wind speed (c,j), depth (e,k) and satellite-derived turbidity (Turb $\log_{10}$ transformed; f,l). Left panels (a-f) represent hydro-sedimentological classes under prevailing conditions, while right panels (g-i) represent classes under extreme event conditions (respectively simultaneous extreme river discharge and potential windburst, extreme river discharge and potential windburst). The shaded upper portion of (a,g) and (d,j) respectively represent the threshold defining occurrence of extreme river discharge ($Q_{log10} > 3.24$ m^3.s^{-1}) and potential windburst events ($U > 6.82$ m.s^{-1}) in the Gironde Estuary. Classes are ordered based on increasing turbidity.

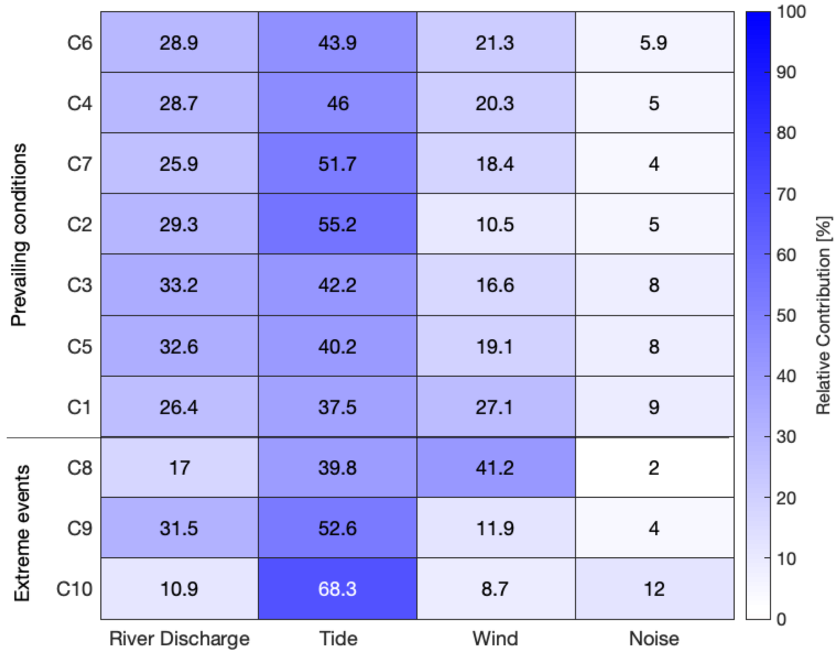

Figure SMG-3 - Class-specific relative contribution (%) of predicting factors (river discharge, tide, wind) for satellite-derived turbidity (database B) and identified uncertainty or noise. Classes C1-C7 depict relative contribution of forcing mechanisms under prevailing conditions (ordered in classes from low (C6) to high (C1) log SSC), classes C8-C10 depict relative contribution of extreme events (extreme high river discharge, potential windbursts, and simultaneous extremes, respectively).